Alginate-modified Cassava Fiber Loaded Palladium for Electochemical Paracetamol Analysis

Haobing Shi[1], Yuhong Zheng[2], Hassan Karimi-Maleh[3,4,5] and Li Fu[1,]*

[1] Key Laboratory of Novel Materials for Sensor of Zhejiang Province, College of Materials and Environmental Engineering, Hangzhou Dianzi University, Hangzhou, 310018, PR. China
[2] Institute of Botany, Jiangsu Province & Chinese Academy of Sciences (Nanjing Botanical Garden Mem. Sun Yat-sen), Nanjing 210014, PR. China
[3] School of Resources and Environment, University of Electronic Science and Technology of China, P.O. Box 611731, Xiyuan Ave, Chengdu, PR. China
[4] Department of Chemical Engineering and Energy, Laboratory of Nanotechnology, Quchan University of Technology, Quchan, Iran
[5] Department of Chemical Sciences (formerly Department of Applied Chemistry), University of Johannesburg, P.O. Box 17011, Doornfontein Campus, Johannesburg 2028, South Africa
[*]E-mail: fuli@hdu.edu.cn

It is required that the content of paracetamol in an individual capsule should not exceed 325 mg, thus the accurate detection of paracetamol content in drugs is essential for controlling the quality of drugs and ensuring the safety of patients. Electrochemical methods are easy to operate and low cost with no requirement of complex pre-treatment, which greatly reduces the detection time. The most widely used electrochemical method for the determination of paracetamol content is the application of the chemically modified electrode. In this work, alginate-modified cassava fibers were adopted as a substrate with palladium immobilized and used for the modification of glassy carbon electrode, and the kinetic processes of paracetamol on the electrode surface and the electrochemical behavior under different pH conditions were investigated. This modified electrode has a very high sensitivity to paracetamol and is capable of making linear detection at 10-370 μM, with the limit of detection calculated to be 1.2 μM.

1. INTRODUCTION

Paracetamol, chemically known as hydroxyphenylacetamide, is a commonly used antipyretic and analgesic drug of the acetanilide class. Over a century of development, paracetamol has been increasingly and widely used, being the top one antipyretic and analgesic in the international

pharmaceutical market [1–3]. The antipyretic effect of paracetamol is similar to that of aspirin, but the analgesic effect is weaker, without the anti-inflammatory and anti-rheumatic effect. It is the best acetanilide drug, especially for patients who cannot use carboxylic acid drugs. Paracetamol has gradually become a substitute for finasteride because of its lower side effects compared with those of finasteride [4]. It is mainly used in clinical practice for the treatment of fever, headache and post-surgical pain. Since 1966, when Prescott first reported a severe liver damage due to paracetamol overdose [5], studies on its toxicity have been emphasized. In recent years, paracetamol has been reported to be a risk factor for asthma, allergic diseases and stroke [6–11]. The latest FDA regulations require that for an individual capsule, the content of paracetamol cannot exceed 325 mg. Accurate detection of paracetamol content in drugs is of great importance for controlling the quality of drugs and ensuring the safety of patients.

Several methods have been widely adopted for the determination of paracetamol in drugs, including spectrophotometry, high performance liquid chromatography (HPLC), capillary electrophoresis, flow injection chemiluminescence, fluorescence and electrochemical methods [12–21]. Spectrophotometry is a method for qualitative and quantitative analysis of a substance by measuring the absorption of light at a specific wavelength or in a certain wavelength range, which has the advantages of high sensitivity, good stability, simple equipment, easy and fast operation as well as wide application. However, the interference of the excipients and degradation products in the paracetamol commercial products will lead to a decrease in the sensitivity of the detection. HPLC is a technique that is commonly used in pharmacological analysis, with a relatively short separation and analysis time, but the sample pretreatment and the selection of operating conditions are time-consuming. An electrochemical sensor is a detection device that applies its internal detection element to detecting chemical signals from external substances. In the case that the target object emits certain chemical signals, they will then be captured by the detection unit inside the sensor, and the detection and analysis will be started.

Direct electrochemical sensors were invented in the middle of the last century and have a high detection accuracy and a relatively simple preparation process. The electrodes of these sensors are mainly prepared from semiconductor or conductor materials, and each electrode has a layer of modification material on its surface, which will directly affect the performance of the sensor. With the excellent catalytic properties, the modification of noble metal nanomaterials to the electrode surface can effectively increase the electron transfer rate, expand the specific surface area of the electrode, and improve the microstructure of the electrode surface [22–27]. The agglomeration of nanomaterials is a problem that needs to be noted, as it can weaken the electrochemical performance. By introducing a substrate to support nanomaterials, the agglomeration of noble metal nanomaterials can be reduced while maintaining a high reactivity.

Cellulose materials are excellent natural polymer materials harboring the most abundant properties. However, deficiencies of these materials also exist, such as low electron mobility and poor electrical conductivity as far as electrode modification materials for electrochemical sensors are concerned [28,29]. Therefore, it is necessary to prepare composite materials with the assistance of modified materials to effectively compensate the deficiency of cellulose in this application and to obtain electrode modification materials with favorable performance.

In this study, the alginate-modified cassava fibers were adopted as a substrate. Afterwards, palladium nanoparticles were loaded onto the surface of the alginate-modified cassava fibers via a wet

chemical method, from which a composite was obtained which possesses both the biocompatibility of plant fibers and the high electron mobility of Pd NPs. By adopting this composite to modify the glassy carbon electrode (GCE), the overpotential of the sensing of paracetamol can be reduced. This analytical tool was used for the electrochemical detection of paracetamol at a very low concentration.

2. MATERIALS AND METHODS

Paracetamol standard solution was prepared in the following steps. First 0.0151g of paracetamol was accurately weighed, and was dissolved with 10 mL of deionized water to make 10 mM of paracetamol solution. It was stored in the refrigerator below 4°C and was diluted to the required concentration when used.

0.2 M phosphate buffer solution (PBS, pH=7.0) was prepared with potassium dihydrogen phosphate and disodium hydrogen phosphate.

The preparation process of palladium nanoparticles and cassava fiber-alginate loaded palladium composites is as follows. 1 g/L ascorbic acid solution was slowly added to 5 mM $PdCl_2$ solution by drops, and the reaction was stirred magnetically at room temperature for 2 h, after which the black particles were centrifuged and washed with deionized water and ethanol solution three times. Finally, 10 mL of deionized water was added to prepare the palladium nanoparticle modification solution. 10 mg of alginate modified cassava fiber powder (Zhejiang Huaxin Agricultural Biotechnology Co., Ltd.) was added to 5 mM $PdCl_2$ solution for 2 h magnetic stirring. Afterwards, 1 g/L ascorbic acid solution was slowly added to mixed dispersion and reacted for 2 h. After centrifugation and washing steps, the cassava fiber-alginate loaded palladium composite was prepared (denoted as PdCF).

The electrode modification process is as follows. The glassy carbon electrode (GCE) was polished with 0.05 μm Al_2O_3, and was rinsed with deionized water and ultrasonically cleaned. 10 mg of modifier was weighed and put into 10 mL of water, and ultrasonically dispersed to produce 1.0 g/L dispersion, after which 5.0 μL of modifier was drop coated on a GCE and dried at room temperature to produce the modified electrode. The PdNPs and PdCF modified GCE were denoted as Pd/GCE and PdCF/GCE, respectively.

3. RESULTS AND DISCUSSION

The effects of different modification materials on the electrode were characterized with $Fe(CN)_6^{3-/4-}$ as a probe. Figure 1a shows CVs of GCE, Pd/GCE and PdCF/GCE in 10 mM $Fe(CN)_6^{3-/4-}$. Neither PdNPs nor PdCF significantly increased the specific surface area of the electrodes, which represents a very limited amount of modification that was performed on the electrode surface. This low amount of modification ensured that the electrode surface did not form a highly thick modification film that would hinder electron migration and in the meantime would not come off during the detection process [30]. However, both PdNPs and PdCF modifications reduced the peak-to-peak separation potential, demonstrating that the modifications improved the electron transfer performance of the electrodes. In contrast, the electrodes modified with PdNPs are superior to PdCF in terms of electron transfer

performance, the reason for which may be the non-conductivity of cassava fibers, with a clearer distinction in the representation of EIS. As shown in Figure 1b, the EIS plots of GCE exhibit the largest semicircle, indicating that it has the highest impedance. In contrast, both PdNPs and PdCF-modified GCEs shows smaller semicircles, indicating that their impedances were reduced. The PdCF-modified GCE has a larger radius than the PdNPs-modified GCE, indicating that PdCF is not superior to PdNPs in terms of electrical properties, which is common in the synthesis of cellulose-based catalysts. Although the composite material is inferior to the pure metal catalyst in terms of electrical properties, the composite catalyst will excel in catalytic performance due to the support provided by the cellulose [31,32].
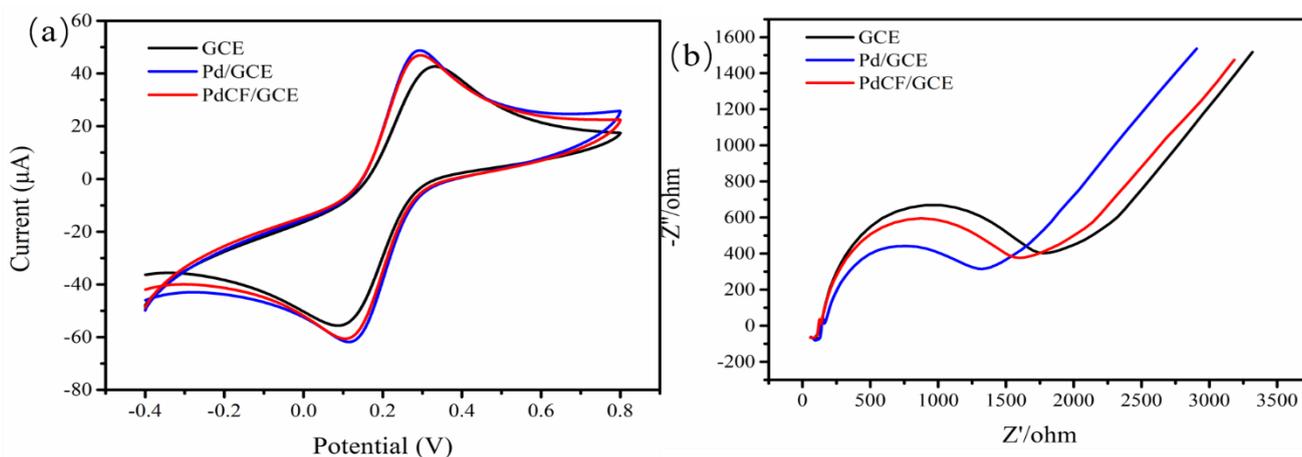
Figure 1. (a) Cyclic voltammograms and (b) Nyquist plots of GCE, Pd/GCE and PdCF/GCE toward 10 mM $Fe(CN)_6^{3-/4-}$ and 0.1 M KCl (pH 7).

After the above process, the response of GCE, Pd/GCE and PdCF/GCE to paracetamol was investigated. Figure 2 shows the CV plots of GCE, Pd/GCE and PdCF/GCE in PBS with the presence of 80 μM paracetamol. It can be noted that the GCE has a clear electrochemical oxidation peak, located at 0.57 V. Since glassy carbon does not react electrochemically in this electrochemical window, it can be determined that this oxidation peak is the oxidation of paracetamol.
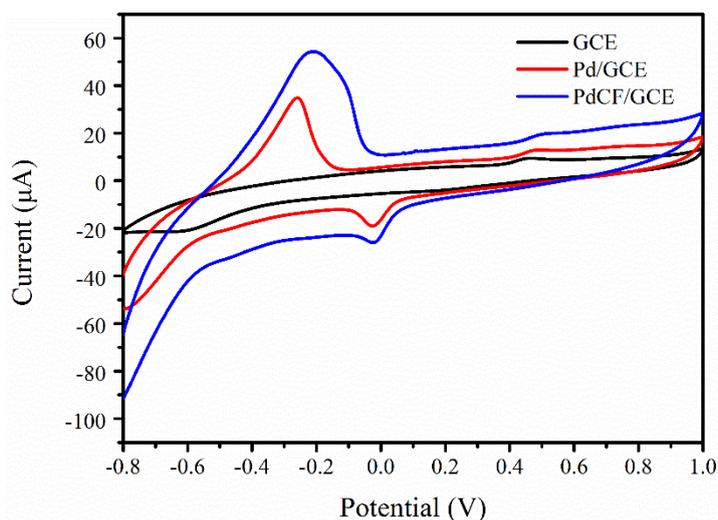
Figure 2. Cyclic voltammograms of GCE, Pd/GCE and PdCF/GCE toward 80 μM paracetamol in PBS (pH 7).

The PdNPs-modified GCE also has an electrochemical oxidation peak at the same position. In contrast, the electrochemical oxidation current of Pd/GCE is higher than that of GCE, representing that the modification of PdNPs could enhance activity the corresponding to paracetamol. In addition, Pd/GCE has a pair of redox peaks at 0.03 V and -0.31 V, which is the conversion between metallic Pd and oxidized Pd state [33–35]. PdCF/GCE is the most sensitive of all electrodes to paracetamol. It can be seen that the electrochemical oxidation current of PdCF/GCE for 80 μM paracetamol is more than twice that of GCE.

The pH of the electrolyte affects the response performance of the sensor. To investigate the effect of pH of PBS on PdCF/GCE, PBS solutions with pH=5.0, 6.0, 7.0, and 8.0 were prepared with 0.2 M KH_2PO_4 (pH=4.5) and 0.2 M Na_2HPO_4 (pH=9.0). Figure 3a shows the cyclic voltammetry curves of PdCF/GCE in PBS buffer solutions of different pH containing 80 μM paracetamol. The potential of the oxidation peak shifted in the negative direction as the pH increased. It can be seen from the figure that the response of PdCF/GCE to paracetamol was maximum at pH 7.0, thus pH=7.0 PBS solution was chosen as the supporting electrolyte for this experiment. Figure 4b presents that the oxidation peak potential of paracetamol on PdCF/GCE shows a positive linear relationship with pH, and the linear equation is $E_{pc} = -0.05949$ pH $+ 0.8937$. The slope of 0.0595 mV/pH is close to the theoretical value of 0.059 mV/pH, indicating that the reaction of paracetamol on PdCF/GCE was a process involving equal electrons and equal protons [36–38].
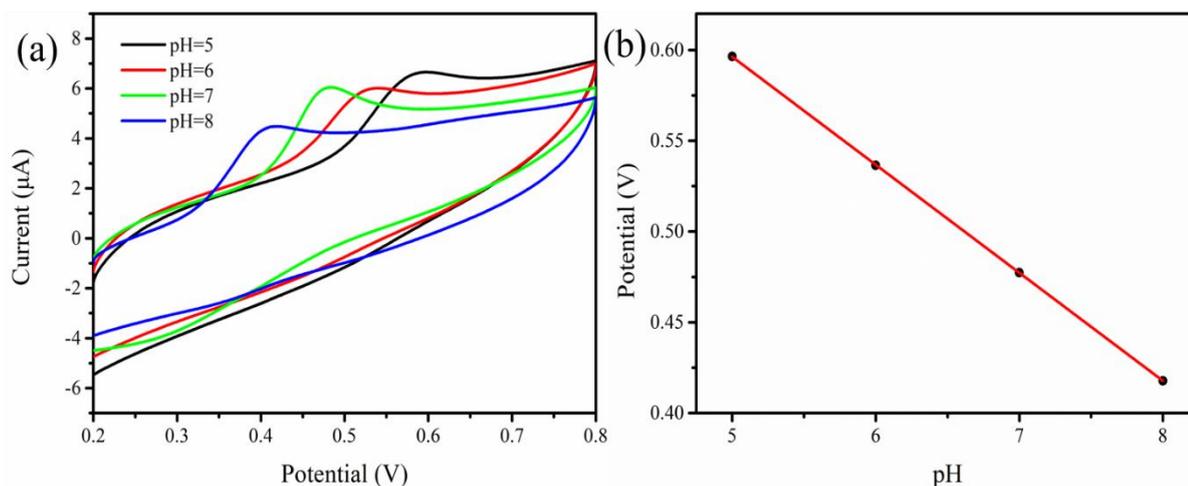
Figure 3. (A) Cyclic voltammograms of PdCF/GCE toward 80 μM paracetamol in PBS with different pH conditions. (B) Plots of oxidation potentials vs. pH conditions.

The effect of different scan rates on the electrochemical behavior of 80 μM paracetamol is shown in Figure 4. It can be noted that the peak increases gradually when the scan rate is from 20 mV/s to 200 mV/s (Figure 4a). A linear relationship between the peak current and scan rate can be found in Figure 4b. The linear equation is: $I_{pc} = 0.04529v + 1.05167$ ($R^2 = 0.98141$), which indicates that the electrode process is controlled by the adsorption process [39–41]. According to Laviron's theory [42], the electron transfer number of paracetamol reacting on PdCF/GCE can be derived from the following equation:

$$Ip = \frac{n^2 F^2 A \Gamma T v}{4RT} = \frac{nFQv}{4RT}$$

Where n is the number of electron transfer, F is the Faraday constant, A is the electrode surface area, Γ is the adsorption amount, R is the molar gas constant, T is the thermodynamic temperature, $Q = nFA\Gamma$ is the peak area, and v is the scan rate. When the scan rate v = 0.1 V/s, the number of electron transfer of the electrode reaction according to the peak is n≈1. Thus the reaction of tea polyphenols on PdCF/GCE is single electron and proton transfer process.
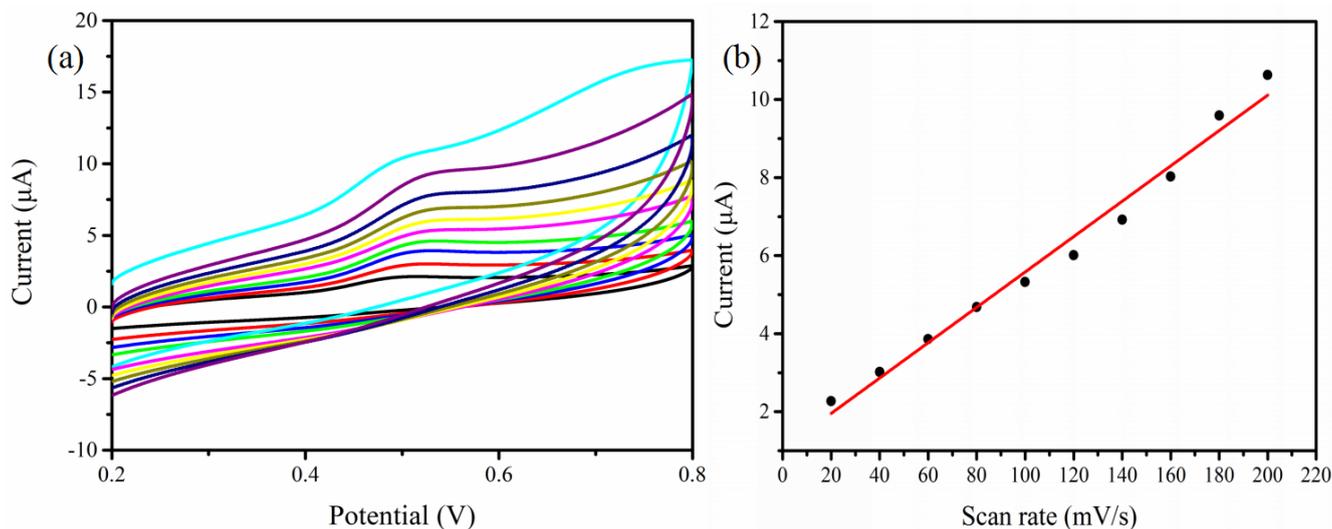
Figure 4. (A) Cyclic voltammograms of PdCF/GCE toward 80 μM paracetamol in PBS using 20 mV/s-200 mV/s. (B) Plots of oxidation currents vs. scan rate.

Figure 5 shows the DPV curves of different concentrations of paracetamol on PdCF/GCE. The oxidation peak current gradually increased in the range of 10 μM-370 μM, showing a linear relationship with the concentration. The linear equation was I(μA) = 0.01361 c+1.23955 (R^2=0.99973) with a detection limit of 2.4 μM (S/N=3). Table 1 shows the comparison of analytical performance with that in previous literature. It can be seen that the proposed PdCF/GCE has exhibited an excellent sensing performance compared with previous reports.
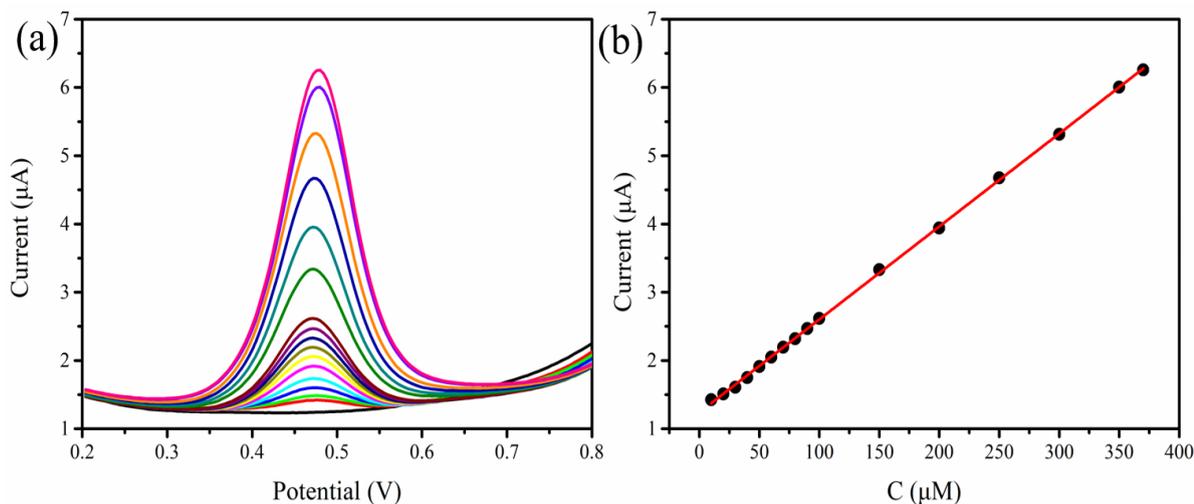
Figure 5. (a) DPV profiles of PdCF/GCE toward paracetamol from 10 μM to 370 μM in PBS (pH 7). (b) Plots of paracetamol concentrations against peak currents.

Table 1. Comparison of previously reported paracetamol electrochemical sensor with this work.

Electrode	Detection method	LR	LOD	Ref
Paracetamol Ab/GO	SWV	0.17 to 10 μM	0.17 μM	[43]
FeS-NPs/ERGO/GCE	DPV	5 to 300 μM	0.18 μM	[44]
Graphene/chitosan	DPV	1 to 100 μM	0.3 μM	[45]
MWCNTs/poly(amidoamine)	DPV	0.3 to 200 μM	0.1 μM	[46]
TiO_2-GR	DPV	1 to 100 μM	0.21 μM	[47]
Graphene oxide	DPV	0.05 to 1 μM	0.049 μM	[48]
NiONPs-CB-DHP/GCE	DPV	3 to 47.8 μM	0.12 μM	[49]
$NeCeO_2$@rGO	CV	0.05 to 0.60 μM	0.0098 μM	[50]
MWCNTs/PoPD/PT	DPV	0.2 to 40 μM	0.05 μM	[51]
MIP/GO/GCE	DPV	0.1 to 80 μM	0.02 μM	[52]
3D AuPd/GN-CNTs-IL	DPV	0.1 to 10 μM	50 nM	[53]
PdCF/GCE	DPV	10 to 370 μM	1.2 μM	This work

4. CONCLUSIONS

The detection of paracetamol is of great significance in the field of pharmacology. In this work, an electrochemical sensor was proposed for the efficient detection of paracetamol. Alginate modified cassava fibers were used as a substrate. PdNPs were anchored onto alginate-modified cassava fibers by a wet chemical method, from which a composite was obtained which requires only a small amount to improve the performance of glassy carbon electrodes and to detect paracetamol by electrochemical oxidation. We also optimized the detection parameters and investigated the electrode kinetic mechanism. This sensor provides linear detection of paracetamol from 10 to 370 μM with a calculated detection limit of 1.2 μM. It is believed that this electrochemical sensor has great potential for future use in the field of healthcare for its rapid detection and ease of operation.

References

1. A.F. Streit, G.C. Collazzo, S.P. Druzian, R.S. Verdi, E.L. Foletto, L.F. Oliveira, G.L. Dotto, *Chemosphere*, 262 (2021) 128322.
2. B. Nadolny, R.G. Heineck, H.A.G. Bazani, J.V. Hemmer, M.L. Biavatti, C.M. Radetski, G.I. Almerindo, *J. Environ. Sci. Health Part A*, 55 (2020) 947–956.

3. M. Culebras, M. Pishnamazi, G.M. Walker, M.N. Collins, *Molecules*, 26 (2021) 1593.
4. T.A. Ahmed, K.M. El-Say, K.M. Hosny, B.M. Aljaeid, *Drug Dev. Ind. Pharm.*, 44 (2018) 652–661.
5. J.S. Thomson, L. Prescott, *Br. Med. J.*, 2 (1966) 506.
6. A. Feola, B. Della Pietra, *Acta Medica Mediterr.*, 33 (2017) 55–58.
7. J. Żur, D. Wojcieszyńska, K. Hupert-Kocurek, A. Marchlewicz, U. Guzik, *Chemosphere*, 206 (2018) 192–202.
8. M. El-Boshy, M.A. BaSalamah, J. Ahmad, S. Idris, A. Mahbub, A.H. Abdelghany, R.A. Almaimani, H. Almasmoum, M.M. Ghaith, M. Elzubier, *Free Radic. Biol. Med.*, 141 (2019) 310–321.
9. N. El Menyiy, N. Al-Waili, A. El Ghouizi, W. Al-Waili, B. Lyoussi, *Nutr. Res. Pract.*, 12 (2018) 535.
10. L. Fadda, H.M. Ali, G.A. Aldrees, N.M. Alquraishi, *Toxicol. Rep.*, 6 (2019) 712–717.
11. L. Zhang, Z. Ren, Z. Su, Y. Liu, T. Yang, M. Cao, Y. Jiang, Y. Tang, H. Chen, W. Zhang, *J. Clin. Endocrinol. Metab.*, 106 (2021) 988–998.
12. J. Huang, J. Tong, J. Luo, Y. Zhu, Y. Gu, X. Liu, *ACS Sustain. Chem. Eng.*, 6 (2018) 9760–9770.
13. X. Liu, W. Na, H. Liu, X. Su, *Biosens. Bioelectron.*, 98 (2017) 222–226.
14. K. Tan, Q. Ma, J. Luo, S. Xu, Y. Zhu, W. Wei, X. Liu, Y. Gu, *Biosens. Bioelectron.*, 117 (2018) 713–719.
15. N. Wester, J. Etula, T. Lilius, S. Sainio, T. Laurila, J. Koskinen, *Electrochem. Commun.*, 86 (2018) 166–170.
16. G. Ibáñez-Redín, D. Wilson, D. Gonçalves, O. Oliveira Jr, *J. Colloid Interface Sci.*, 515 (2018) 101–108.
17. S.M. Azab, *J. Electroanal. Chem.*, 840 (2019) 319–327.
18. M.M. Charithra, J.G. Manjunatha, *J. Electrochem. Sci. Eng.*, 10 (2020) 29–40.
19. R. Mangaiyarkarasi, S. Premlatha, R. Khan, R. Pratibha, S. Umadevi, *J. Mol. Liq.*, 319 (2020) 114255.
20. L. Fu, A. Wang, G. Lai, C.-T. Lin, J. Yu, A. Yu, Z. Liu, K. Xie, W. Su, *Microchim. Acta*, 185 (2018) 1–7.
21. N. Kumar, A.S. Bhadwal, B. Mizaikoff, S. Singh, C. Kranz, *Sens. Bio-Sens. Res.*, 24 (2019) 100288.
22. A. Abellán-Llobregat, C. González-Gaitán, L. Vidal, A. Canals, E. Morallon, *Biosens. Bioelectron.*, 109 (2018) 123–131.
23. S. Kempahanumakkagari, A. Deep, K.-H. Kim, S.K. Kailasa, H.-O. Yoon, *Biosens. Bioelectron.*, 95 (2017) 106–116.
24. S. Kempahanumakkagari, K. Vellingiri, A. Deep, E.E. Kwon, N. Bolan, K.-H. Kim, *Coord. Chem. Rev.*, 357 (2018) 105–129.
25. I. Bolat, A. Ikinci, *Fresenius Environ. Bull.*, 29 (2020) 1542–1549.
26. H. Kir, *Fresenius Environ. Bull.*, 20 (2020) 2843–2849.
27. F. Kizilgeci, N.E.P. Mokhtari, A. Hossain, *Fresenius Environ. Bull.*, 29 (2020) 8592–8599.
28. G. Li, K. Sun, D. Li, P. Lv, Q. Wang, F. Huang, Q. Wei, *Colloids Surf. Physicochem. Eng. Asp.*, 509 (2016) 408–414.
29. P. Phukon, K. Radhapyari, B.K. Konwar, R. Khan, *Mater. Sci. Eng. C*, 37 (2014) 314–320.
30. R. Yang, B. Fan, S. Wang, L. Li, Y. Li, S. Li, Y. Zheng, L. Fu, C.-T. Lin, *Micromachines*, 11 (2020) 967.
31. G.-Y. Hou, Z.-Y. Lyu, Y.-P. Tang, H.-Z. Cao, G.-Q. Zheng, *Int. J. Hydrog. Energy*, 45 (2020) 16049–16059.
32. L. Wei, J. Luo, L. Jiang, L. Qiu, J. Zhang, D. Zhang, P. Xu, D. Yuan, *Int. J. Hydrog. Energy*, 43 (2018) 20704–20711.
33. Z. Karimi, M. Shamsipur, M.A. Tabrizi, S. Rostamnia, *Anal. Biochem.*, 548 (2018) 32–37.

Int. J. Electrochem. Sci., 16 **(2021)** Article Number: 21108

10

34. P.A. Rasheed, R.P. Pandey, K.A. Jabbar, J. Ponraj, K.A. Mahmoud, *Anal. Methods*, 11 (2019) 3851–3856.
35. T. Wu, T. Li, Z. Liu, Y. Guo, C. Dong, *Talanta*, 164 (2017) 556–562.
36. C. Costentin, M. Robert, J.-M. Savéant, *Acc. Chem. Res.*, 43 (2010) 1019–1029.
37. L. Chen, Y. Tang, K. Wang, C. Liu, S. Luo, *Electrochem. Commun.*, 13 (2011) 133–137.
38. C. Costentin, *Chem. Rev.*, 108 (2008) 2145–2179.
39. A.M. Fathi, H.S. Mandour, E. HassaneAnouar, *J. Mol. Struct.*, 1224 (2021) 129263.
40. K. Chetankumar, B.K. Swamy, *Sens. Int.*, 1 (2020) 100001.
41. P.T. Pınar, S. Allahverdiyeva, Y. Yardım, Z. Şentürk, *Microchem. J.*, 155 (2020) 104772.
42. Ejj. Laviron, *J. Electroanal. Chem. Interfacial Electrochem.*, 101 (1979) 19–28.
43. M. Tertiş, O. Hosu, L. Fritea, C. Farcau, A. Cernat, R. Săndulescu, C. Cristea, *Electroanalysis*, 27 (2015) 638–647.
44. X. Liu, E. Shangguan, J. Li, S. Ning, L. Guo, Q. Li, *Mater. Sci. Eng. C*, 70 (2017) 628–636.
45. M. Zheng, F. Gao, Q. Wang, X. Cai, S. Jiang, L. Huang, F. Gao, *Mater. Sci. Eng. C*, 33 (2013) 1514–1520.
46. Y. Zhang, X. Liu, L. Li, Z. Guo, Z. Xue, X. Lu, *Anal. Methods*, 8 (2016) 2218–2225.
47. Y. Fan, J.-H. Liu, H.-T. Lu, Q. Zhang, *Colloids Surf. B Biointerfaces*, 85 (2011) 289–292.
48. M. Zidan, R.M. Zawawi, M. Erhayem, A. Salhin, *Int J Electrochem Sci*, 9 (2014) 7605–7613.
49. P. Batista Deroco, F. Campanhã Vicentini, O. Fatibello-Filho, *Electroanalysis*, 27 (2015) 2214–2220.
50. S.K. Ponnaiah, P. Prakash, B. Vellaichamy, *Ultrason. Sonochem.*, 44 (2018) 196–203.
51. Y. Peng, Z. Wu, Z. Liu, *Anal. Methods*, 6 (2014) 5673–5681.
52. J. Luo, J. Cong, R. Fang, X. Fei, X. Liu, *Microchim. Acta*, 181 (2014) 1257–1266.
53. L. Yang, B. Zhang, B. Xu, F. Zhao, B. Zeng, *Talanta*, 224 (2021) 121845.